

# Tunneling spectroscopy of midgap states induced by arsenic precipitates in low-temperature-grown GaAs

R. M. Feenstra, A. Vaterlaus,<sup>a)</sup> J. M. Woodall, and G. D. Pettit  
IBM Research Division, T. J. Watson Research Center, Yorktown Heights, New York 10598

(Received 7 June 1993; accepted for publication 24 August 1993)

The scanning tunneling microscope is used to study arsenic precipitates in low-temperature-grown and annealed GaAs. Tunneling spectroscopy reveals a distribution of states throughout the band gap, arising from the precipitates, with the density of midgap states increasing as the precipitate size increases. The Fermi level is found to be pinned at  $E_V + 0.65$  eV for 600 °C annealed material. For 800 °C annealed material the Fermi level is located at  $E_V + 1.05$  eV in regions far from precipitates, and additional depletion regions are observed near the precipitates.

The properties of GaAs grown at low temperatures near 200 °C have been the subject of numerous recent studies.<sup>1-8</sup> The as-grown material is known to contain an excess arsenic concentration of about 2 at. %, leading to a concentration of point defects (mainly arsenic antisite defects) of about  $1 \times 10^{20}$  cm<sup>-3</sup> (Refs. 2 and 3). Subsequent annealing causes this excess arsenic to agglomerate and form precipitates.<sup>4,5</sup> In both the as-grown and the annealed material, the Fermi level is generally found to be pinned near midgap, leading to relatively high resistivities which are useful for device applications.<sup>1</sup> For as-grown material this pinning is attributed to the arsenic-related point defects, but for annealed material some controversy has arisen as to the relative role of the arsenic precipitates in the pinning compared to that of residual point defects.<sup>6,7</sup>

In this work, we present spectroscopy results acquired with a scanning tunneling microscope (STM) on low-temperature-grown and annealed (LTA) GaAs. Measurements have been performed on material annealed at 600 and 800 °C, and precipitates are observed with diameters of about 50 and 150 Å, respectively. In both cases, a distribution of states throughout the band gap is found to be induced by the arsenic precipitates, with the density of states at the precipitates being higher for the 800 °C case. The Fermi level for the 600 °C annealed material is found to be pinned at  $E_V + 0.65$  eV throughout the LTA layer, whereas for the 800 °C case a Fermi-level position of  $E_V + 1.05$  eV is found far from the precipitates with additional depletion regions observed near the precipitates. The existence of midgap states associated with the precipitates demonstrates that they are, in principle, capable of pinning the Fermi level. Furthermore, the observation of depletion regions around the precipitates for the 800 °C annealed material (far separated precipitates) demonstrate that they do indeed play a role in the Fermi-level pinning. Some residual pinning between the precipitates is observed, and possible sources of this pinning are discussed below.

The LTA-GaAs was grown at 225 °C, in a Varian Gen-II molecular-beam epitaxy system. Annealing was performed *in situ* at 600 °C for 30 min under an As pres-

sure of  $10^{-6}$  Torr, and in some cases additional annealing was performed *ex situ* at 800 °C for 30 s. The LTA layers are *n*-type, doped with Si at a concentration of  $1 \times 10^{19}$  cm<sup>-3</sup>, and have thickness of typically 500 Å. These layers are surrounded on both sides by 500-Å-thick *p*-type layers (Be doped at  $5 \times 10^{19}$  cm<sup>-3</sup>) grown at 350 °C, which serve as markers for the LTA layer, and *n*-type layers (Si-doped at  $1 \times 10^{19}$  cm<sup>-3</sup>) grown at 350–600 °C surround the *p*-type layers. The samples were cleaved in the STM ultrahigh-vacuum chamber with base pressure of  $< 4 \times 10^{-11}$  Torr. The cleavage procedure, and details of the STM design, are described elsewhere.<sup>8</sup> STM images were obtained with a constant tunnel current of 0.1 nA, and at various voltages specified below. Spectroscopic measurements were performed using a method previously developed for obtaining a large dynamic range in the tunnel current and conductivity.<sup>9</sup>

Figure 1 shows STM images obtained from the LTA-GaAs annealed at 600 °C, showing topography and conductance in Figs. 1(a) and 1(b), respectively. As marked in the conductance image, the LTA layer extends over

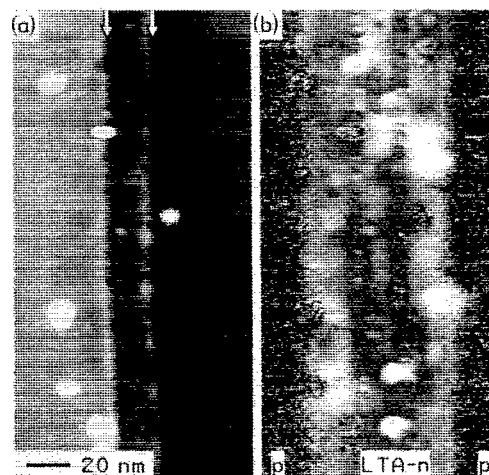


FIG. 1. STM image of a cleaved GaAs structure, showing (a) topography and (b) conductivity, acquired at a sample voltage of  $-2.5$  V. The grey-scale range in (a) is 8 Å. As indicated in (b), the structure contains a LTA *n*-type layer, surrounded by *p*-type layers grown at higher temperature. The sample was annealed at 600 °C. Two steps occur in the LTA layer, as marked by arrows in (a).

<sup>a)</sup>Permanent address: FKP-Mikrostrukturforschung, ETH Hoenggerberg, HPT C2.2, 8093 Zurich, Switzerland.

most of the image, with the neighboring  $p$  layers seen at the right- and left-hand sides of the image. Two steps occur on the cleavage face in the LTA layer, as marked by the arrows at the top of Fig. 1(a), and these steps lead to some local pinning of the Fermi level as seen by the dark lines occurring at the same spatial location in Fig. 1(b). Small protrusions can be seen in the LTA layer, appearing as white circular areas in Fig. 1(a). These protrusions have typical diameter of about 50 Å and height of 15 Å (the observed diameter is sometimes larger due to tip convolution effects; the 50 Å value is derived from measurements with relatively sharp probe tips). Such protrusions are never seen on  $n$ - or  $p$ -type material grown at temperatures of 350 °C or higher, and thus we identify the protrusions with the arsenic precipitates which are known to occur in this material.<sup>4,5</sup> In addition to the precipitates present in Fig. 1(a), several depressions or "holes" are visible in the image, appearing as the dark circular areas with typical diameter of 50 Å. We associate these holes with regions where an arsenic precipitate has been pulled out of the material during the cleave. (In general, one expects the same number of protrusions as depressions in the images.) Based on the observed number of protrusions and holes, we estimate a precipitate density of  $12 \times 10^{16} \text{ cm}^{-3}$ , in reasonable agreement with that found in transmission electron microscopy (TEM) studies.<sup>6</sup>

In Figs. 2(a) and 2(b), respectively, we show STM topographic and conductance images obtained from LTA-GaAs annealed at 800 °C. The LTA layer extends over most of the imaged area, as marked at the bottom of Fig. 2(b). Several cleavage steps are visible in the topography, and these steps give rise to some local Fermi-level pinning as seen by the darker areas in the conductance image. A large precipitate is observed near the center of Fig. 2(a); line cuts through this precipitate at the location indicated by the arrows are shown in Fig. 2(c), and discussed in detail below. Some holes have also been observed on this LTA layer, although they are not visible in Fig. 2(a) because of the large grey-scale range required for displaying the precipitate. Much fewer precipitates are observed in the 800 °C annealed material compared to the 600 °C case; we estimate a precipitate density of about  $7 \times 10^{15} \text{ cm}^{-3}$  with a precipitate diameter of about 150 Å.

The states introduced into the GaAs band gap by the precipitates are shown in the tunneling spectra of Figs. 3(a) and 3(b), for the 600 and 800 °C annealed material, respectively. Spectra shown with dashed lines were acquired on the LTA-GaAs layer at a position in between precipitates, and spectra shown with solid lines were acquired directly on the precipitates. The GaAs spectra display a well defined band-gap region, with width equal to the bulk gap of 1.43 eV. The position of the Fermi level corresponds to 0 V in the spectra, yielding Fermi-level positions far from the precipitates of  $E_V + 0.65 \text{ eV}$  and  $E_V + 1.05 \text{ eV}$  for Figs. 3(a) and 3(b), respectively. For the precipitate spectrum of Fig. 3(a), tails of states can be seen extending into the band-gap region. These states are most pronounced on the conduction-band side, but can also be seen on the valence-band side. The density of midgap states

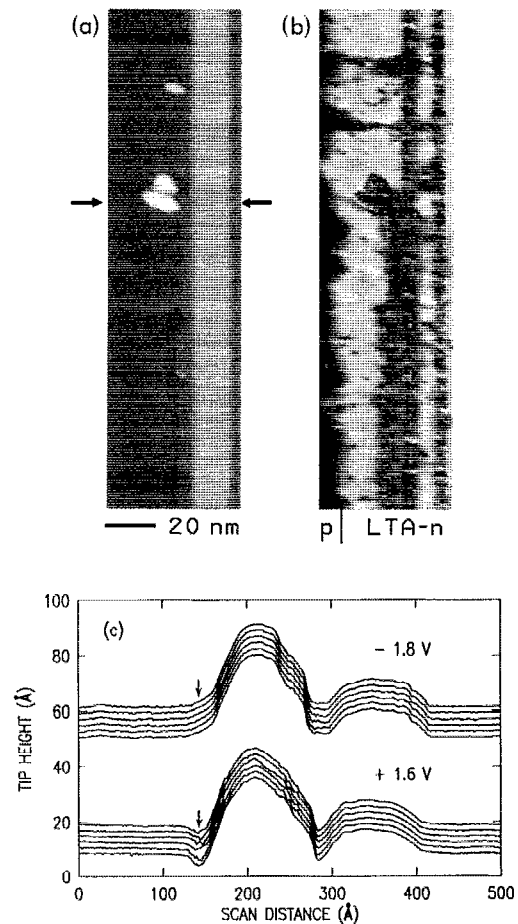


FIG. 2. STM image of a cleaved GaAs structure, showing (a) topography and (b) conductivity, acquired at a sample voltage of  $-2.3 \text{ V}$ . The grey-scale range in (a) is 33 Å. As indicated in (b), the structure contains a LTA  $n$ -type layer, bordered on the left-hand side by a  $p$ -type layer grown at higher temperature. The sample was annealed at 800 °C. Cross-sectional cuts along the line indicated by arrows in (a) are displayed in panel (c), acquired at sample voltages of  $-1.8$  and  $+1.6 \text{ V}$ .

observed in Fig. 3(a) is small; orders-of-magnitude below that of an ideal metal. We attribute this low density to the small size (50 Å), of the precipitates, keeping in mind that bulk arsenic itself is only a semimetal. In Fig. 3(b), the number of midgap states introduced by the precipitates has greatly increased, with an average value of  $(dI/dV)/(I/V)$  throughout the gap nearly equal unity, indicating good metallic behavior. A small gap of width 0.5 eV is still observed in the state density on the precipitates, and oscillations in the spectrum are seen at higher voltages. We tentatively attribute both of these observations to quantum size effects of the precipitates, although a structural transition observed between small and large precipitates<sup>10</sup> may also affect their electronic properties.

According to the model for Fermi-level pinning in LTA-GaAs proposed by Warren *et al.*<sup>4,6</sup> the precipitates are responsible for the pinning, and for far separated precipitates the Fermi level should return to its band-edge location in regions between the precipitates thereby creating depletion spheres around each precipitate. For the present case of  $1 \times 10^{19} \text{ cm}^{-3}$   $n$ -type doping, the width of these spheres around each precipitate is predicted to be

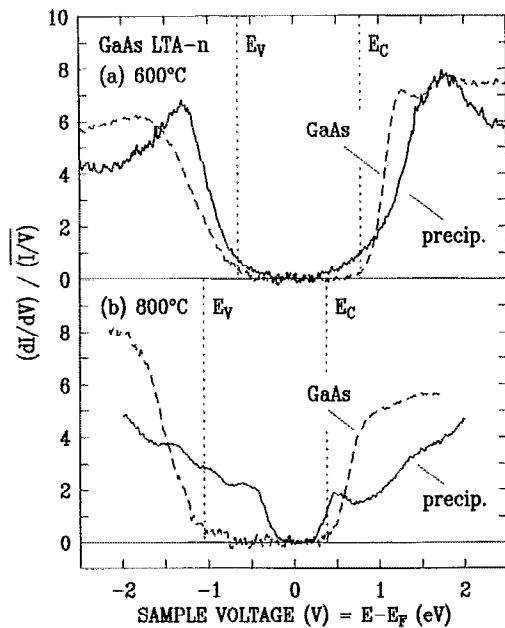


FIG. 3. STM spectra acquired from the LTA *n*-type layers, annealed at (a) 600 and (b) 800 °C. Spectra are shown acquired on the arsenic precipitates (solid line) and on regions of bare GaAs in between the precipitates (dashed line). The valence- and conduction-band edges are marked by  $E_V$  and  $E_C$ , respectively.

about  $\sqrt{(2\epsilon\phi/e^2N)} = 100 \text{ \AA}$  for barrier height of  $\phi = 0.7 \text{ eV}$  and dielectric constant of  $\epsilon = 12.9$ . In Figs. 1(b) or 2(b), these depletion spheres would appear as reduced conductance (darker regions) around the precipitates, and such effects are not clearly evident in the images. For the case of Fig. 1, the precipitate separation may be small enough to prevent complete formation of the depletion spheres, but for Fig. 2 the precipitate separation is much greater than the  $100 \text{ \AA}$  depletion width. However, if we look more closely at the large precipitate imaged in Fig. 2, we can observe the formation of a depletion region around it, as shown in Fig. 2(c). The line cuts in Fig. 2(c) were acquired across the precipitate, using sample voltages of  $-1.8$  and  $+1.6 \text{ V}$ . At the edge of the precipitate, as marked by the arrows in Fig. 2(c), we observed at negative bias a region of increased tip height (i.e., increased tunnel current) and at positive bias this same region shows decreased tip height. The voltage dependence of this feature demonstrates that it is a purely electronic effect, and indeed, this type of behavior is precisely what occurs for local depletion around a charged metal island.<sup>11</sup> The range of the depletion seen in Fig. 2(c) is about  $25 \text{ \AA}$ , significantly less than the depletion width of  $100 \text{ \AA}$  predicted above. One reason for this reduction is that the barrier height around the precipitate is smaller since we observe a Fermi-level position of  $E_V + 1.05 \text{ eV}$ , i.e., not completely at the conduction-band edge. We do not know why perfectly flat-band conditions are not observed between precipitates, although a small amount of surface band bending may occur in the LTA-layers (a few steps are always seen in those layers). Another possible reason for the observed small depletion width is that the nonzero size of the STM

probe-tip itself makes it difficult to measure right up to the edge of the precipitate.

In summary, we have used the STM to study the electrical properties of arsenic precipitates in LTA-GaAs. We observe a significant density of midgap states induced by the precipitates, thereby demonstrating that they are capable of pinning the Fermi level in this material. We also observe local depletion around the precipitates, indicating that they are charged and thus indeed are responsible (at least in part) for determining the Fermi level position in this material. It has been proposed that point defects in LTA-GaAs may play an important role in the Fermi level pinning. The importance of point defects depends on their concentration relative to the shallow dopant concentration. For the present case of highly doped *n*-type material, a concentration of residual acceptor defects approaching  $10^{19} \text{ cm}^{-3}$  is required to significantly affect the Fermi level position. Such a high concentration of point defects is not directly seen in our work, and is orders of magnitude higher than that expected on the basis of other studies,<sup>7</sup> so we consider it unlikely that point defects affect the Fermi level position in these materials. Nevertheless, a residual concentration of acceptors could determine the Fermi-level position for lower doped *n*-type material, and it is important to obtain a direct measure of this point defect concentration. Additional studies, over a wider range of shallow dopant concentrations and growth temperatures, are currently in progress in an effort to further elucidate the role of arsenic precipitates compared with point defects in determining the Fermi-level position of LTA-GaAs.

We thank M. R. Melloch for useful discussions throughout the course of this work. One of us (A.V.) gratefully acknowledges financial support from the Swiss National Fund.

<sup>1</sup>F. W. Smith, A. R. Calawa, C. L. Chen, M. J. Mantra, and L. J. Mahoney, *IEEE Electron Device Lett.* **9**, 77 (1988).

<sup>2</sup>M. Kaminska, Z. Liliental-Weber, E. R. Weber, T. George, J. B. Kortright, F. W. Smith, B.-Y. Tsaur, and A. R. Calawa, *Appl. Phys. Lett.* **54**, 1881 (1989).

<sup>3</sup>See, e.g., M. Kaminska and E. R. Weber, *Mater. Sci. Forum* **83-87**, 1033 (1992), and references therein.

<sup>4</sup>A. C. Warren, J. M. Woodall, J. L. Freeouf, D. Grischkowsky, D. T. McInturff, M. R. Melloch, and N. Otsuka, *Appl. Phys. Lett.* **57**, 1331 (1990).

<sup>5</sup>Z. Liliental-Weber, G. Cooper, R. Mariella, and C. Kocot, *J. Vac. Sci. Technol. B* **9**, 2323 (1991).

<sup>6</sup>A. C. Warren, J. M. Woodall, P. D. Kirchner, X. Yin, F. Pollack, M. R. Melloch, N. Otsuka, and K. Mahalingam, *Phys. Rev. B* **46**, 4617 (1992).

<sup>7</sup>D. C. Look, *J. Appl. Phys.* **70**, 3148 (1991).

<sup>8</sup>A. Vaterlaus, R. M. Feenstra, P. D. Kirchner, J. M. Woodall, and G. D. Pettit, *J. Vac. Sci. Technol. B* **11**, 1502 (1993).

<sup>9</sup>P. Mårtensson and R. M. Feenstra, *Phys. Rev. B* **39**, 7744 (1988).

<sup>10</sup>Z. Liliental-Weber, G. Cooper, R. Mariella, and C. Kocot, *J. Vac. Sci. Technol. B* **9**, 2323 (1991).

<sup>11</sup>J. A. Stroschio, R. M. Feenstra, D. M. Newns, and A. P. Fein, *J. Vac. Sci. Technol. A* **6**, 499 (1988); R. M. Feenstra and P. Mårtensson, *Proceedings of the 19th International Conference on the Physics of Semiconductors*, edited by W. Zawadzki (Polish Institute of Physics, Warsaw, 1988).